Preparation of Nb-doped PZT Thin Film with High Piezoelectric Performance and Its Application to MEMS Devices

Takamichi FUJII*, Takayuki NAONO*, Akihiro MUKAIYAMA*, Takami ARAKAWA*,
Yoshikazu HISHINUMA**, Youming LI**, and Jeffrey BIRKMEYER**

Abstract

We have developed a method of forming PZT films on silicon substrates with a high piezoelectric coefficient using RF sputtering. Films have been formed on 6-inch wafers with thickness variation of less than +/− 5% across the entire wafer. Our PZT film has an unusually high content of Nb dopant (13%) which results in 1.7-fold higher piezoelectric coefficient than sputtered PZT films previously reported. The X-ray diffraction patterns of our PZT film formed on a 6-inch wafer demonstrate that the film is in a perovskite phase with (100) orientation which partly accounts for its high piezoelectric performance. One of the unique properties of our sputtered PZT film can be observed in the P-E hysteresis loop shifted to the positive electric field, suggesting that the polarization axes have been aligned in a certain direction beforehand, making a post-deposition polarization process unnecessary. We applied the PZT film to an ink-jet head and micro-mirror as a MEMS device application, and demonstrated high actuation performances of both devices.

1. Introduction

The actuators of ink-jet heads, etc., use piezoelectric materials for their driving units. To achieve higher definition and higher performance from those devices, it is necessary to refine the actuator mechanisms by applying semiconductor technologies such as microelectromechanical systems (MEMS). To that end, research and development have been undertaken that enable piezoelectric materials to be changed from conventional bulk materials that require polishing to thin films.[1)]

Normally, long-established PZT materials are used for that purpose. The piezoelectric performance (d_{31}) of undoped genuine bulk PZT materials is −93 pm/V and that is not sufficient for actuators. Therefore, in general, third component-added denatured PZT or materials in the relaxor system are used. Among the methods to make piezoelectric materials into thin films are the sol-gel process, sputtering, aerosol deposition and chemical vapor deposition.[2)-9)] To form good-quality films with a high piezoelectric constant, those methods have introduced an annealing step after film deposition or techniques utilizing epitaxial growth with single-crystal substrates to enhance crystallization. Currently, however, films formed on silicon substrates compatible with the MEMS process have not been able to achieve sufficiently high piezoelectric performance.

Therefore, by using sputtering, which is highly versatile and enables easy film formation in the order of micrometers, we formed a PNZT film with a piezoelectric constant enhanced by doping PZT with Nb on a silicon substrate via electrodes. This paper describes the characteristics of that film and its application to MEMS devices.

2. Nb-doped PZT thin film by sputtering[10)-12)]

2.1 Nb-doped PZT thin film

PZT is a complex oxide having a perovskite structure, expressed by the chemical formula $Pb(Zr_xTi_{1-x})O_3$. Fig. 1 illustrates the structure. Pb^{2+} ions are positioned at A sites, and Zr^{4+} or Ti^{4+} ions occupy B sites. At a temperature not greater than the Curie point, B-site ions, Zr^{4+} or Ti^{4+}, shift from the center of the crystal and that causes spontaneous polarization. Those ions undergo a displacement in response to the external electric field, which appear as ferroelectricity and piezoelectricity. In this development, a trial was made to increase the piezoelectric constant with a material created by doping the B sites with Nb (hereinafter, "PNZT").

Original paper (Received December 20, 2013)

* Advanced Marking Research Laboratories
Research & Development Management Headquarters
FUJIFILM Corporation
577 Ushijima, Kaisei-machi, Ashigarkami-gun, Kanagawa
258-8577 Japan

** FUJIFILM Dimatix, Inc.
2230 Martin Avenue, Santa Clara, CA 95050, U.S.A.

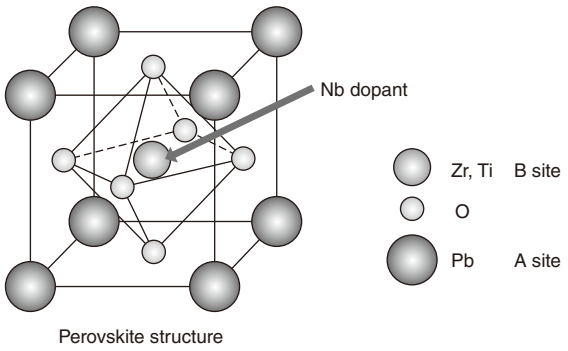

Fig. 1 Crystal structure of PZT.

2.2 Conditions for the forming of a sputtered PNZT thin film and its evaluation method

Using a silicon substrate with a (100) orientation, we formed, as follows, a PNZT thin film with our original RF magnetron sputtering equipment that allows 6-inch film formation. First, a 20-nm Ti adhesion layer was formed on the silicon substrate by sputtering. Then, a 150-nm lower Ir electrode was deposited. On that substrate, a PNZT film was formed by sputtering using the $Pb_{1.1}(Zr_{0.46}Ti_{0.42}Nb_{0.12})O_3$ target. The ratio of Zr to Ti in the target was set to 52:48, which is the same as that of the morphotropic phase boundary (MPB). That composition achieves the highest piezoelectric constant and electromechanical coupling coefficient; therefore, it is suitable for actuators. Also, to further improve its piezoelectric properties, we made a 12% doping of the target with Nb (perovskite B-site conversion). Under those conditions and at a deposition temperature between 450 and 550°C, we succeeded in the formation of a stable PNZT film with a perovskite structure.

For the evaluation of the formed PNZT film, we checked its crystal structure and orientation with X-ray diffraction (XRD), observed the cross-sectional structure with a scanning electron microscope (SEM) and a transmission electron microscope (TEM), and performed composition analysis with X-ray fluorescence (XRF). To evaluate its ferroelectric properties, the P-E hysteresis loop was measured and, using an impedance analyzer, the dielectric constant and loss tangent values were measured. In addition, we created a diaphragm structure via micromachining and evaluated the film's mechanical displacement properties by applying a voltage and measuring the magnitude of the resulting displacement with a laser Doppler vibrometer. The piezoelectric constant (d_{31}) was determined via simulation and the value was evaluated with the $e_{31, f}$ measuring equipment (manufactured by aixACCT). For some evaluation items, comparison was made with genuine PZT samples without Nb doping.

2.3 Structure and composition

Fig. 2 shows the results for the XRD measurement of the PNZT film formed on the 6-inch wafer. The measurement positions are at the center of the wafer and at locations 5 cm above, below, to the left and to the right of the center. The observation of the diffraction peaks revealed that the film did not have any peaks other than the perovskite phase. Therefore, it can be said that PNZT with a single-phase perovskite structure was created. With regard to the crystal orientation, only a peak attributable to the (100) orientation appeared, which means the crystal was perfectly oriented in that direction.

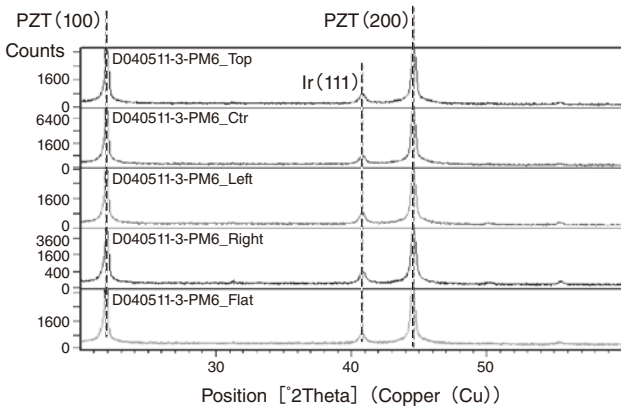

Fig. 2 X-Ray diffraction pattern of PNZT film.

The in-plane composition distribution of the film was also measured with XRF. The results obtained are shown in Table 1, according to which, a PZT film containing approximately 13% Nb was formed evenly on the wafer. While doping general bulk materials with Nb at a concentration of 3% or more may cause separation, form a pyrochlore phase or decrease performance, this film incorporates Nb atoms in without such problems. Under the deposition conditions of this film, doping with an even larger amount of Nb caused cracks on the film. Thus, no higher level of Nb doping was used.

Fig. 3 presents the cross-sectional SEM and TEM images of the obtained film. The film having a columnar structure is densely packed without gaps between grain boundary or at the electrode

Table 1 Composition of 6-inch sputtered PNZT film at 5 locations on a wafer.

Position	Pb/(Zr + Ti + Nb)	Zr/(Zr + Ti)	Ti/(Zr + Ti)	Nb/(Zr + Ti + Nb)
Top	1.096	0.505	0.495	0.130
Left	1.099	0.505	0.495	0.130
Center	1.121	0.506	0.494	0.128
Right	1.085	0.503	0.497	0.130
Flat	1.086	0.502	0.498	0.129

interface. A fine PNZT film was formed from the lower electrode interface.

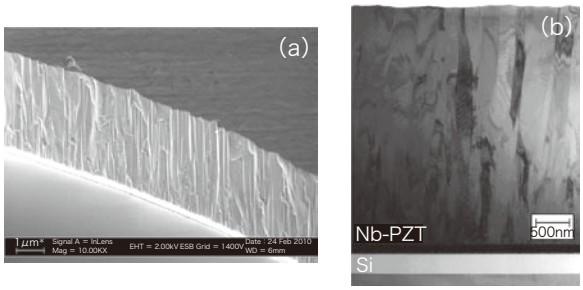

Fig. 3 SEM and TEM images of PNZT cross-sections: (a) SEM image and (b) TEM image.

2.4 Piezoelectric and electrical properties

We formed an upper electrode on the obtained film and measured the P-E hysteresis to evaluate its ferroelectric properties. The results obtained are shown in Fig. 4. For comparison, the data for genuine PZT are also shown. According to the figure, the PNZT film achieved an excellent hysteresis loop, which is significantly shifted to the right, compared with genuine PZT. That means, as one of its major characteristics, the film has a polarized state right from its creation (described later).

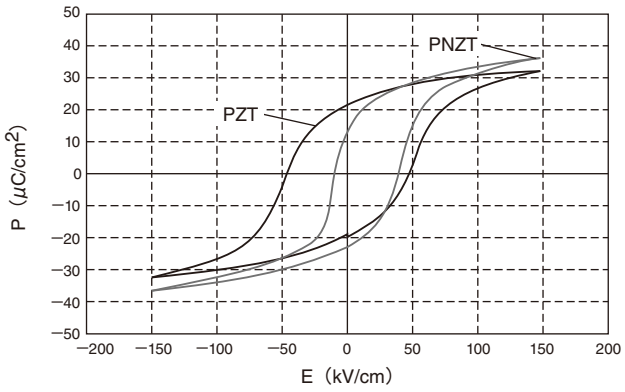

Fig. 4 P-E hysteresis loops of PZT and PNZT.

Table 2 contains the thickness, dielectric constant (ε), loss tangent (tan δ) and maximum value of remanent polarization (P_{rmax}) of the film on the 6-inch wafer. Each property was relatively uniform across the wafer.

Table 2 Film thickness, dielectric constant, tan δ and max. polarization of PNZT film at 5 locations on a wafer.

Position	Thickness (μm)	ε	tan δ	P_{rmax} (μC/cm²)
Top	3.01	1161	0.020	38.8
Left	2.96	1139	0.020	38.9
Center	3.14	1209	0.022	37.6
Right	2.99	1136	0.020	39.4
Flat	3.09	1184	0.020	38.9

2.5 Piezoelectric constant evaluation, drive properties and other properties of the PNZT thin film

To calculate the piezoelectric constant, we created a diaphragm structure as shown in Fig. 5 with MEMS technology and, while applying voltage between the upper and lower electrodes, measured the displacement magnitude at the center of the diaphragm with a laser Doppler vibrometer. Subsequently, the piezoelectric constant, d_{31}, was determined with the finite element method.[10), 11)] For the Young's modulus of the PNZT film, which is an important parameter required for that determination, we used 49GPa calculated from the resonance frequency of the structure. As a result, $d_{31} = -259$ pm/v was obtained for this PNZT film. The value was approximately 1.7 times that of conventional material.

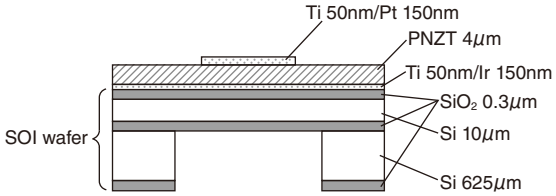

Fig. 5 Schematic of diaphragm structure for displacement measurement.

Separately, we measured the $e_{31,f}$ piezoelectric constant with the four-point bending system aix4PB manufactured by aixACCT Systems. That piezoelectric constant can be evaluated by reading the electrical charges that are generated in the piezoelectric film via the positive piezoelectric effect caused by the application of stress with the four-point bending method to the laminated cantilever of a silicon substrate (25 mm^L × 3 mm^W), lower electrode, piezoelectric film and upper electrode. As shown in Fig. 6, $e_{31,f} = -25.1$ C/m² was obtained for this PNZT film, which is the highest performance for mass-production products currently available.

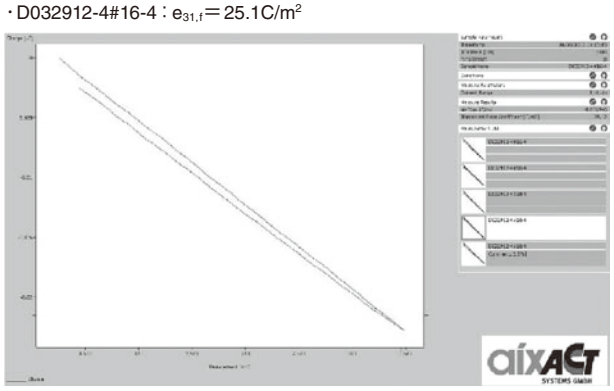

Fig. 6 Piezoelectric coefficient $e_{31,f}$ of PNZT film.

With a diaphragm structure as shown in Fig. 5, we also evaluated the drive properties of the film by applying voltage to the upper electrode and connecting the lower electrode to ground potential. The results obtained are presented in Fig. 7. When negative voltage was applied to the upper electrode of the obtained device, the displacement increased linearly (①) and, as the voltage was reduced, it decreased linearly (②). Next, when positive voltage was applied, the polarity of the piezoelectric material was inverted near its coercive electric field (at approximately 10 V), chang-

ing the direction of displacement, and the displacement became greater with the voltage. Then, as the voltage was reduced, the displacement occurred in the way shown as ④. Although this is not given in Fig. 7, when negative voltage was applied again, the displacement exhibited the same tendency again as shown at ①. Thus, the obtained PNZT film has the characteristic of returning to the previous state immediately even if the polarity is inverted. That is, the PNZT film is a strong spontaneously polarized film, initially in the direction that will achieve excellent displacement with negative drive; therefore, even if it is polarized in the opposite direction, the film is restored to the previous state immediately. Incidentally, because of the dependence of its capacitance on temperature, the Curie point of the film was the same level as general PZT materials (approximately 340°C). Moreover, it was revealed that the PNZT film spontaneously keeps its polarity in the same direction and even if it is heated, it re-polarizes itself.

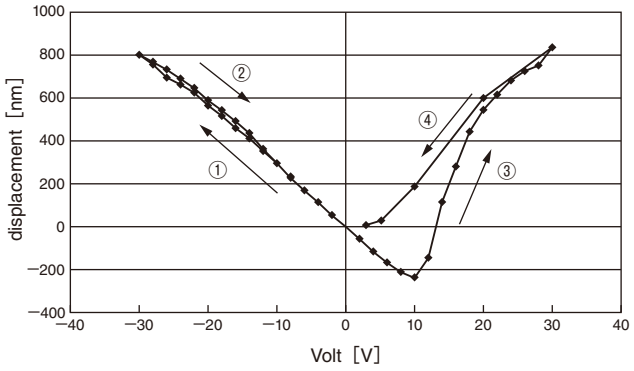

Fig. 7 Displacement of PNZT film.

In summary, the obtained film has the following characteristics: it is pre-polarized immediately after its formation; it is not easily polarized in the direction opposite to its spontaneous polarization; and it restores its polarity even if it is heated. Those characteristics can be considered to be advantageous for the application of the film to devices, indicating that no depolarization occurs even in high-temperature processes such as reflow and no post-deposition polarization process is necessary, and thus they can achieve long-term stable drive performance.

Fig. 8 indicates the I-V properties measured to investigate the breakdown voltage of a 3-μm-thick PNZT film. According to the figure, the breakdown voltage was not smaller than 300 V. The reason for negative voltage being applied was that, as previously described, it was the pre-polarization and actual drive direction of the film: that is, negative voltage was applied to the upper electrode when the lower electrode was connected to ground potential. It can be considered that such a high breakdown voltage is achieved because the film is dense and contains no gaps as shown in Fig. 3. Applying this high breakdown-voltage PNZT film to devices enables drive design with sufficient capacity.

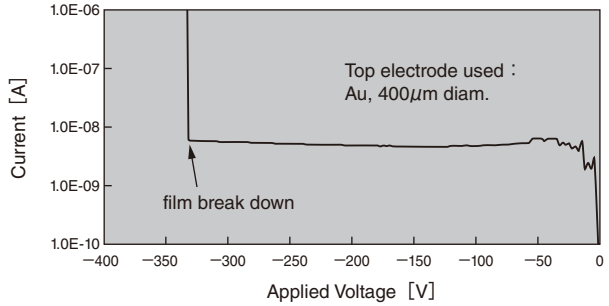

Fig. 8 *I-V* measurement on 3μm-thick PNZT film.

However, because breakdown voltage can be affected by damage via the MEMS formation process, it is necessary to handle the film with care in the process of its application to devices.

3. Application examples

3.1 Application to ink-jet heads

We applied the PNZT film we developed in this research to ink-jet heads. Fig. 9 illustrates the outline drawing of an ink-jet head using a piezoelectric material. Conventional ones are made by polishing a bulk material attached to a silicon substrate. On the other hand, a PNZT film is directly formed via sputtering, which reduces variations in thickness and differences in levels as well as improves homogeneity (Fig. 10). Bulk materials are difficult to handle

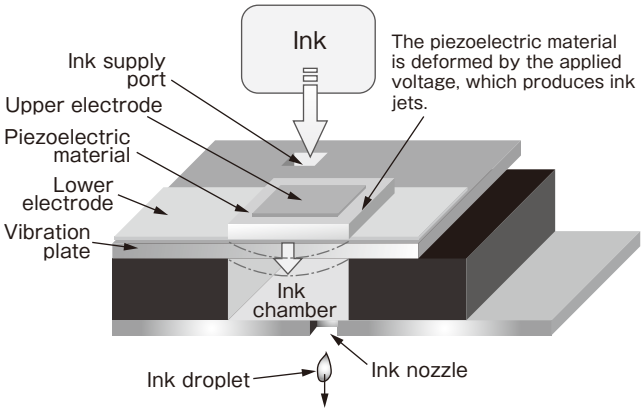

Fig. 9 Image of ink jet head.

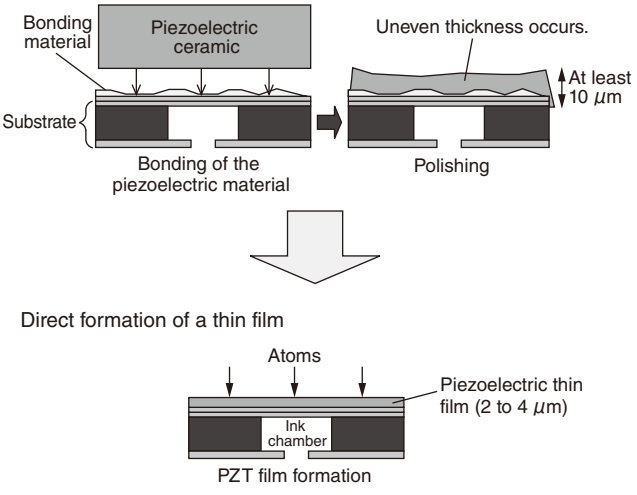

Fig. 10 Process of fabricating ink jet heads using bulk PZT and thin-film PZT.

because they can be depolarized and thus their polarization quality degrades considerably after reflow. However, as already described, this PNZT film does not need a post-deposition polarization process and does not change with heat; therefore, it is highly durable and can provide a technological margin for process conditions.

Fig. 11 presents a photo of a head module manufactured by FUJIFILM Dimatix using this PNZT film. Having incorporated MEMS technology, the ink-jet head realized a resolution of 1,200 dpi, droplet volume of 2 pL, 2,048 nozzles/inch, frequency of 100 kHz and high durability. Thus, it has an extensive range of uses.

Fig. 11 MEMS ink jet head“SAMBA”.

3.2 Application to micromirrors

Drive methods for micro scanners are divided into the following four categories: electrostatic; electromagnetic; thermoelectric; and piezoelectric. Each method has its own advantages but the piezoelectric method seems particularly promising because it can be applied to a variety of uses, achieving a large driving force, in spite of its compact size and relatively low voltage requirements.[13] As part of medical applications, FUJIFILM has already developed micromirrors for incorporation into endoscopes.[14] Fig. 12 shows a conceptual image of the obtained device and a photo of the MEMS mirror. Being held with meandering hinges associated with the cantilever structures driven at both ends, the mirror rotates as the cantilevers move up and down. The drive properties of the device can be changed by altering the thickness, width and number of turning paths of the hinges.

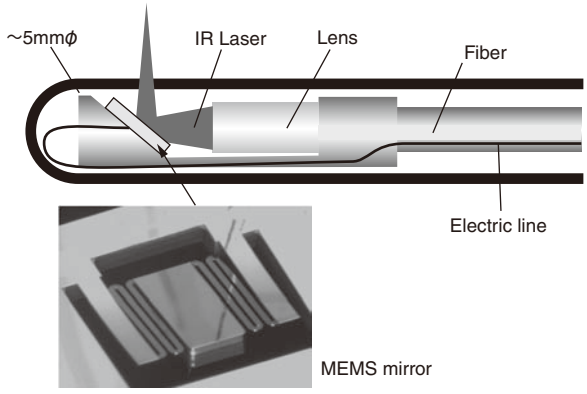

Fig. 12 Typical OCT probe with MEMS scanner.

Fig. 13 indicates the drive properties of the above described device when it uses a PNZT film and a genuine PZT material, each with and without polarization. According to the figure, the device using genuine PZT achieved an optical scan angle of approximately 19° without polarization (as-deposition state) at a drive voltage of 0.5 V. With polarization, the angle greatly increased and an optical scan angle of approximately 43° was achieved at the same drive voltage. That means, the genuine PZT film requires polarization. On the other hand, the one using a PNZT film achieved an optical scan angle of approximately 128° at the same drive voltage, regardless of polarization.

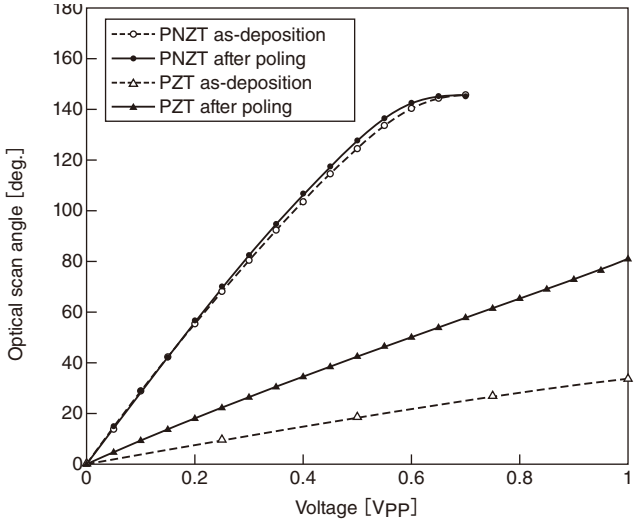

Fig. 13 Voltage response of the micro mirror driven by PNZT and PZT thin films.

The results confirmed that the PNZT film we developed has a larger piezoelectric constant than conventional genuine PZT materials and does not require polarization.

As regards MEMS mirrors, we created some other structures with different resonance frequencies and evaluated their drive frequencies and optical scan angles. To compare the performance with conventional methods including piezoelectric, electromag-

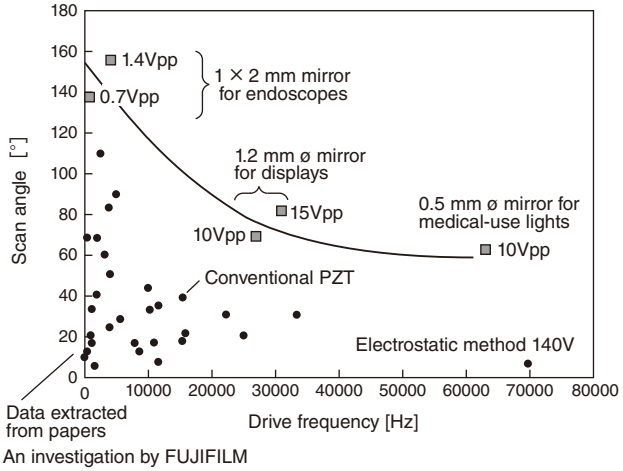

Fig. 14 Comparison of micro mirror performance based on the literature.

netic and electrostatic techniques, data cited from other papers are plotted together in Fig. 14.[15)-22)] In general, the higher the drive frequency, the smaller the scan angle of the mirror becomes. Therefore, as a whole, the higher the drive frequency, the smaller the scan angle becomes. For this research, we developed three types of mirrors: the above described low-speed mirror for endoscopes (resonance frequency of approximately 100 Hz); a middle-speed mirror for displays (approximately 25 kHz); and a high-speed mirror intended for medical, fast wavelength-swept devices (approximately 65 kHz). Each mirror achieved a larger scan angle than the values reported for conventional ones. We believe that it happened because the performance of the PNZT piezoelectric material used as their drive source is superior to conventional ones.

The overall results confirmed that, by using our PNZT film in combination with MEMS technology, it is possible to create higher-performance MEMS mirrors than ever. We are planning to develop products with higher added value by further improving the performance of the piezoelectric film and designing devices that make the most of its characteristics.

4. Conclusion

We formed an Nb-doped PZT film (PNZT film) on a 6-inch wafer via sputtering and evaluated its properties. The PNZT film thus obtained achieved piezoelectric constants, d_{31} and $e_{31,f}$, of −250 pm/V and −25.1 C/m^2 respectively, which proves that the performance of the film is much higher than conventional genuine PZT materials. Across the 6-inch plane, the film exhibited excellent structure and homogeneity in its film thickness and composition. In addition, it was confirmed that the film requires no polarization process because it is pre-polarized immediately after its deposition.

We created an ink-jet head with that PNZT film, realizing high resolution, high-speed printing and high reliability. Moreover, in its application to MEMS micromirrors, having achieved larger scan angles than conventional products, we are convinced that it can be developed for use with various-purpose mirrors.

The PNZT film we developed has unconventionally excellent properties. We will seek to advance that technology into various useful devices, while combining MEMS technology compatible with it and will thereby present new values in society.

References

1) Muralt, P. J. Micromech. Microeng. **10** (2), p.136 (2000)
2) Wolf, R. A.; Trolier-McKinstry, S. J. Appl. Phys. **95** (3), p.1397-1406 (2004)
3) Ledermann, N.; Muralt, P.; Baborowski, J.; Forester, M.; Pellaux, J. P. J. Micromech. Microeng. **14** (12), p.1650 (2004)
4) Sakashita, Y.; Ono, T.; Segawa, H.; Tominaga, K.; Okada, M. J. Appl. Phys. **69** (12), p.8352-8357 (1991)
5) Shimizu, M.; Fujisawa, H.; Shiozaki, T. J. Cryst. Growth. **174**, p.464-472 (1997)
6) Takayama, R.; Tomita, Y. J. Appl. Phys. **65** (4), p.1666-1670 (1989)
7) Kanno, I.; Kotera, H.; Wasa, K.; Matsunaga, T.; Kamada, T.; Takayama, R. J. Appl. Phys. **93** (7), p.4091-4096 (2003)
8) Lebedev, M.; Akedo, J. Jpn. J. Appl. Phys. **41**, p.6669-6673 (2002)
9) Shepard, J. F. Jr.; Chu, F.; Kanno, I.; Trolier-McKinstry, S. J. Appl. Phys. **85** (9), p.6711-6716 (1999)
10) Fujii, T.; Hishinuma, Y.; Mita, T.; Arakawa, T. Solid State Commun. **149** (41), p.1799-1802 (2009)
11) Fujii, T.; Hishinuma, Y.; Mita, T.; Nakano, T. Sens. Actuators A. **163** (1), p.220-225 (2010)
12) Hishinuma, Y.; Li, Y.; Birkmeyer, J.; Fujii, T.; Nakano, T.; Arakawa, T. Nanotechnology 2012 Electronics, Devices, Fabrication, MEMS, Fluidics and Computation: Technical Proceedings of the 2012 NSTI Nanotechnology Conference and Expo Volume 2. Santa Clara, 2012-06-18/21. NTIS, CRC Press, 2012, 878p., 978-1-4665-6275-2.
13) Wolter, Alexander; Hsu, Shu-Ting; Schenk, Harald; Lakner, Hubert. Proc. SPIE. **5719**, MOEMS and Miniaturized Systems V, p.64-75 (2005)
14) Naono, T.; Fujii, T.; Esashi, M.; Tanaka, S. J. Micromech. Microeng. (In press).
15) Smits, J. G.; Fujimoto, K.; Kleptsyn, V. F. J. Micromech. Microeng. **15** (16), p.1285 (2005)
16) Ohtsuka, Y.; Nishikawa, H.; Koumura, T.; Akita, S.; Hattori, T. Denkigakkai Ronbunshi E (IEEJ Transaction on Sensors and micromachines). **116** (8), p. 345-352 (1996)
17) Tsaur, J.; Zhang, L.; Maeda, R.; Matsumoto, S.; Khumpuang, S. Jpn. J. Appl. Phys. **41**, p.4321-4326 (2002)
18) Nippon Signal Co., Ltd. http://www.signal.co.jp/vbc/mems/ecoscan/, (reference, 2014-02-12).
19) Asai, N.; Matsuda, R.; Watanabe, M.; Takayama, H.; Yamada, S.; Mase, M.; Shikida, M.; Sato, K.; Lebedev, M.; Akedo, J. Proceedings of the IEEE International Conference on Micro Electro Mechanical Systems (MEMS) 02/2003. Kyoto, 2003-01-19/23, IEEE, 2003, p.247-250.
20) Isamoto, K.; Totsuka, K.; Suzuki, T.; Sakai, T.; Morosawa, A.; Chong, C.; Fujita, H.; Toshiyoshi, H. 2011 International Conference on Optical MEMS and Nanophotonicstonic. Istanbul, Turkey, 2011-08-8/11. OMN. IEEE, 2011, p.73.
21) Wine, D. W.; Helsel, M. P.; Jenkins, L.; Urey, H.; Osborn, T. D. Proc. SPIE. **4178**, MOEMS and Miniaturized Systems, p.186-196 (2000)
22) Filhol, F.; Defay, E.; Divoux, C.; Zinck, C.; Delaye, M. T. Sens. Actuators A. **123**, p.483-489 (2005)

Trademarks